

THE CHARACTERIZATION OF SEMICONDUCTOR GRAIN  
BOUNDARIES USING VOLUME-INDEXED SURFACE  
ANALYSIS TECHNIQUES.

Lawrence L. Kazmerski  
Solar Energy Research Institute  
Golden, CO 80401, U.S.A.

A new supporting surface analytical method, **Volume-Indexed SIMS**, which facilitates the analysis of the compositional species at internal portions and inter-faces in semiconductor materials and devices, is introduced. The technique indexes the data for mass species, spatial location within a selected volume, and for level or concentration. The utility of this method is demonstrated for the evaluation of the chemistry of impurity interactions at grain boundaries in polycrystalline silicon, including the behavior of hydrogen at these intercrystalline defects.

Surface Analysis, Grain Boundaries

1. Introduction

Impurities, either purposely-placed or incorporated as unwanted artifacts during processing, are known to control the operational characteristics of semiconductor devices<sup>1-3</sup>. This is especially true of impurities accumulated at internal interfaces (such as charge-separating junctions and defects) within the device structure. The ability to model such semiconductor devices, to predict performance and to account for degradation and reliability limitations, depends not only on the knowledge of their possible existence, but also on the exact determination of their type, concentration, spatial location, distribution, and chemistry.

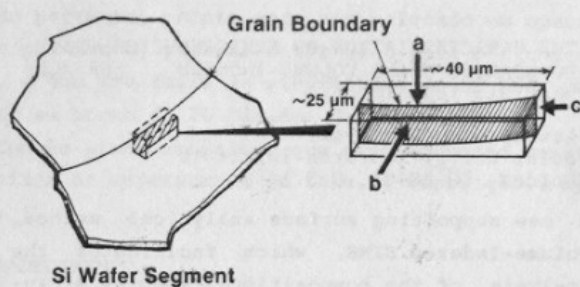


Fig. 1. Representation of Volume-Indexed SIMS technique.

### Volume-Indexed SIMS

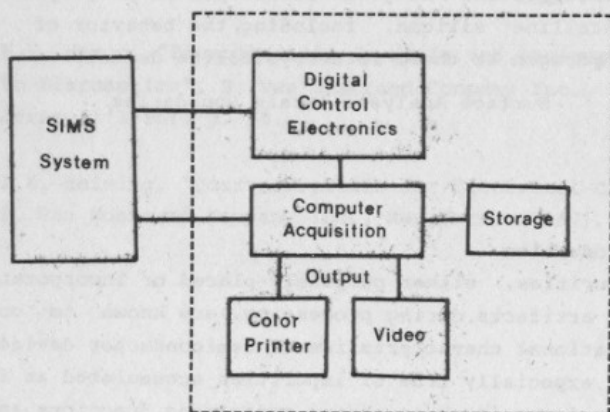


Fig. 2. Block diagram of Volume-Indexed SIMS system.

Several methods are currently used routinely to examine such impurity problems. The combination of surface analytical techniques, such as Auger electron spectroscopy (AES) and X-ray photoelectron spectroscopy (XPS) with sputter ion-etching, dynamic secondary ion mass spectrometry (SIMS), and Rutherford backscattering spectroscopy (RBS) can provide useful compositional information as functions of depth into the device<sup>4-6</sup>. However, such information is essentially confined a region around a line, perpendicular to the surface of the structure under analysis. Thus, it is difficult to observe variations in composition, such as impurity segregation and diffusion, along planes that may be at some angle or parallel to the surface of the device. Attempts to expose internal surfaces using in-situ fracturing techniques have been partially successful in the past<sup>7</sup>. However, these are highly destructive and do not allow for subsequent processing (such as temperature treatments), are probabilistic in exposing the exact area of interest, and may lose the part of the plane containing the desired information of interest to the bottom of the analysis chamber. This paper describes a new technique which facilitates the analysis of compositional species at internal portions and interfaces in semiconductor devices. The utility of the method is exemplified for an important technical problem, the evaluation of the chemistry of impurity interactions at grain boundaries in polycrystalline Si. Specifically, the technique is used to evaluate the electronic passivation of these internal defects by treatment in hydrogen.

## 2. Volume-Indexed SIMS

A representation of the technique is presented in Fig. 18. A commercial SIMS system, either quadrupole or magnetic sector analyzer-based, serves as the basic analysis equipment, and the volume-indexed technique is gained by addition of some control hardware and data collection/processing software (see block diagram of Fig. 2). The incident ion beam impinges on a relatively large area of the sample, usually more than 50  $\mu\text{m}$  by 50  $\mu\text{m}$ . The mass analyzer is controlled to gather information digitally (with approx-

imately 0.5  $\mu\text{m}$  resolution) from a smaller volume, such as that shown in Fig. 1. This volume spatial information is stored during the analysis. The operator can select several mass species for detection, and specify a threshold for detection. Therefore, the data can be indexed for elemental or molecular species and for the relative concentration of that species. Once the data are stored, the software allows the researcher to view those data at any point, along any line or over any plane within the volume analyzed. The planar mapping is particularly useful for the study of chemical interactions at internal device interfaces. Finally, the technique also permits the color coding of the information output as functions of the elemental or molecular type and its concentration level.

### 3. Experimental Details

The base polycrystalline Si used in these studies was produced by casting<sup>9</sup>. The hydrogen passivation technique and relevant heat treatments and processing have been described previously<sup>10-12</sup>. The Volume-Indexed SIMS analyses were performed in a Cameca IMS-3f ion microprobe, but similar data have been obtained on a PHI SIMS II, using a quadrupole mass analyzer.

### 4. Discussion of Hydrogen Passivation

The direct observation of the penetration of hydrogen down grain boundaries has been previously reported<sup>12</sup>. Dube et al. have used EBIC to show the effectiveness of these impurity treatments on cell performance<sup>13</sup>. The activation of grain boundaries has been shown to be a function of the heat treatment of the device, and the segregation of oxygen to the boundary has been identified as a possible source of the minority carrier loss<sup>14</sup>. The interaction between the oxygen present at the defect and the hydrogen diffused into the region has been speculated. However, no conclusion on the chemical reactions between these species have been formulated. Studies that require impurity mapping at internal device interfaces--such as this one--are ideal candidates for the application of the volume-indexing technique.

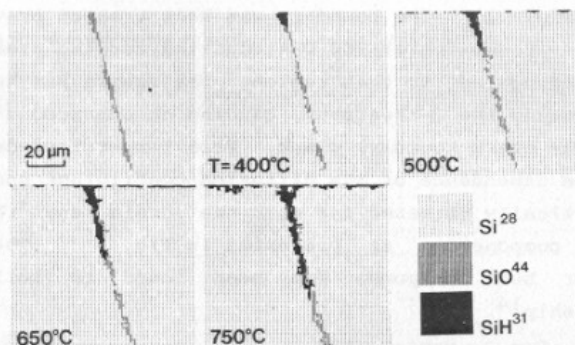


Fig. 3. Volume-Indexed SIMS mapping sequence showing penetration of hydrogen down Si grain boundary. Shown from aspect "c" indicated in Fig. 1.

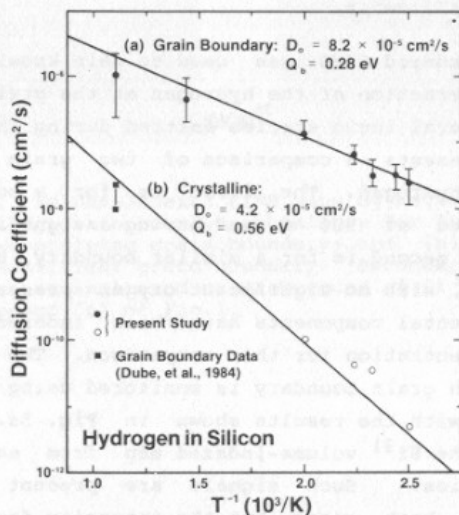


Fig. 4. Diffusion coefficients of hydrogen in Si as a function of inverse temperature: (a) grain boundary diffusion; (b) grain or crystalline diffusion.

The penetration of hydrogen down grain boundaries is illustrated in Fig. 3, with the boundary shown from aspect "c" of Fig. 1. The boundary was heat treated previous to hydrogen processing at 900 C accounting for the presence of oxygen segregated to that region. The sample was heated to 600 C during the H-treatment, causing an enhanced diffusion along the grain boundary plane. From temperature-dependent data, the dependence of the diffusion coefficient upon T can be analytically obtained for both the grain and the grain boundary components, as presented in Fig. 4<sup>14</sup>. The intra-grain or bulk component has been found to follow the relationship<sup>14</sup>,

$$D = D_0 \exp(-Q_b/kT) \quad (1)$$

with  $D_0 = 4.2 \times 10^{-5} \text{ cm}^2/\text{s}$  and  $Q_b = 0.56 \text{ eV}$  (which are consistent with values found in the literature). The grain boundary diffusion is found to be several orders of magnitude greater, fitting the function,  $D' = 8.2 \times 10^{-5} \exp(-0.28 \text{ eV}/kT) \text{ cm}^2/\text{s}$ .

Volume-Indexed SIMS was used to gain knowledge of the chemical interaction of the hydrogen at the grain boundary, tracking several ionic species emitted during the analysis. Figure 5 presents a comparison of two grain boundaries process with hydrogen. The first is for a boundary initially annealed at 900 C and having a significant oxygen content. The second is for a similar boundary, but not heat treated (i.e., with no significant oxygen presence). The ionic or elemental components have been indexed for both type and concentration for this comparison. The oxygen content of each grain boundary is monitored using the  $\text{SiO}^{44}$  SIMS signal, with the results shown in Fig. 5a. Figure 5b represents the  $\text{Si}^{31}$  volume-indexed map from each of the grain boundaries. Such signals are present in the SIMS spectra from both cases, but the intensity from the grain boundary having no oxygen content is an order of magnitude higher (i.e.,  $8 \times 10^{19}$  vs.  $6 \times 10^{18} \text{ cm}^{-3}$  on the average). Complementing these data, the evolution of the  $\text{SiOH}^{45}$  SIMS ionic species is shown for the two grain boundaries in Fig.



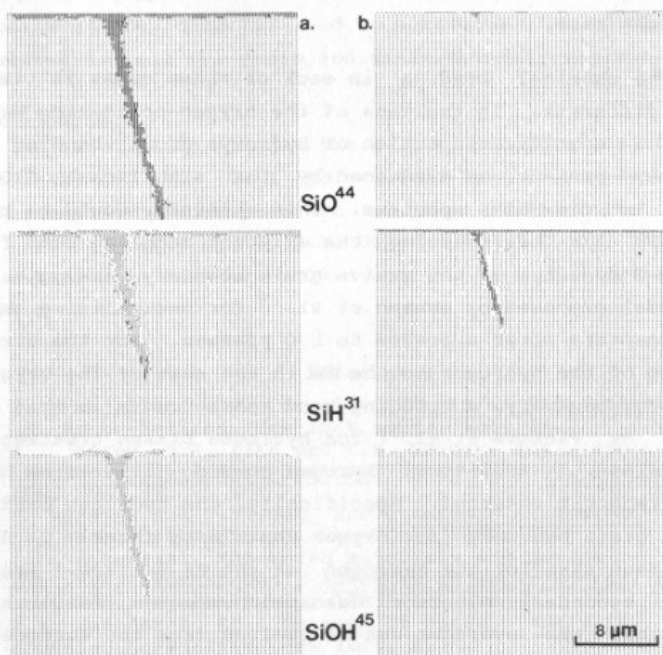


Fig. 5. Volume-Indexed SIMS mapping sequences indicating grain boundary chemistry for (a) oxygen-containing grain boundary; and, (b) oxygen-deficient grain boundary. Secondary ion species are indicated on background of  $\text{Si}^{28}$ . Shown from aspect "c" of Fig.1.

5c. A high secondary ion yield, averaging more than  $5 \times 10^{19} \text{ cm}^{-3}$  is observed in the oxygen containing grain boundary, with no signal detected in the corresponding oxygen-deficient case.

The chemical bonding in each of these cases is likely quite different. In the case of the oxygen-containing boundary, a significant portion of hydroxyl-group bonding is probably present, as evidenced by the significant  $\text{SiOH}^{45}$  signal in the SIMS spectrum. This chemistry would be responsible for neutralizing the existent dangling bond from the Si-O reaction at the active grain boundary, analogous to the model proposed by Hansen et al.<sup>15</sup> for neutralizing shallow acceptors after exposure to H O plasmas. For the direct bonding of the hydrogen to the Si in the case of the oxygen-deficient boundary, a bridging-bond scheme, such as that reported by Pankove et al.<sup>16</sup> for hydrogen plasma treatments, is possible. Additional hydrogen bonding differences have been recently observed. Specifically, the hydrogen bonding in the grain boundary (for oxygen containing cases) is different than that for the hydrogen at the Si surface. Recent oxygen secondary electron desorption studies (ESD) have shown that the hydrogen can be evolved from the surface at temperatures in the range 300-350 C. At the same time, the oxygen at the boundary, even on surfaces exposed by fracture during the ESD experiments, are bound more tightly--even to temperatures beyond 550 C. This difference in bonding is explained by the Volume-Indexed SIMS data of Fig. 5, which shows that the majority of the hydrogen at the surface is bonded directly to the Si, while that at the boundary is bonded through the oxygen. Parallel experiments on oxygen-free boundaries show that the oxygen deep into the inter-grain region evolves at the lower temperature--indicative of the Si-H bonding scheme.

## 6. Summary

A new technique has been discussed which allows the investigation of impurity effects at internal device interfaces, reproducibly and with a single analytical operation. The Volume-Indexed SIMS technique is demonstrated using the



passivation of polycrystalline grain boundaries using hydrogen treatments. The data are utilized to produce a series of molecular maps illustrating the chemical reactions at the intercrystalline defects, and to determine the diffusion parameters in both the grain and grain boundary regions.

### Acknowledgements

The author acknowledges the help and suggestions of his co-workers in the SERI Photovoltaic Devices and Measurements Branch in the preparation of this manuscript. This work was supported by the U.S. Department of Energy through a subcontract to the Solar Energy Research Institute (DE-AC02-83CH10093).

### References

1. S. Mahajan and J.W. Corbett, Defects in Semiconductors II, North-Holland, New York, 1983, Vol. 14.
2. H.J. Leamy, G.E. Pike and C.H. Seager, Eds., Grain Boundaries in Semiconductors, North-Holland, New York, 1982, Vol. 5.
3. J. Narayan and T.Y. Tan, Eds., Defects in Semiconductors, North-Holland, New York, 1981, Vol. 2.
4. L.L. Kazmerski, "Advanced Materials and Device Analytical Techniques", Advances in Solar Energy, K. Boer, Ed., Plenum Press, 1985 (in-press).
5. A.W. Czanderna, Ed., Methods of Surface Analysis, Elsevier Scientific, New York, 1975.
6. W.-K. Chu, J.W. Mayer and M.A. Nicolet, Backscattering Spectroscopy, Academic Press, New York, 1978.
7. L.L. Kazmerski, J. Vac. Sci. Technol. 20 (1982) 423.
8. L.L. Kazmerski, Proc. 17th IEEE Photovoltaic Spec. Conf., IEEE, New York, 1984, pp. 379-385.
9. T.F. Ciszek, G.H. Schwuttke and K.H. Yang, J. Cryst. Growth 46 (1979) 527.
10. R.H. Micheels, Z. Vayman and J. Hanoka, Appl. Phys. Lett. 46 (1985) 414.
11. C.H. Seager, J. Appl. Phys. 52 (1982) 3960.
12. L.L. Kazmerski, Proc. 6th European Photovoltaic Solar Energy Conf., London, Reidel, The Netherlands, 1985 (in-press).
13. C. Dube, J.I. Hanoka and D.B. Sandstrom, Appl. Phys. Lett. 44 (1983) 425.
14. L.L. Kazmerski, J. Vac. Sci. Technol. A3 (1985) 1287.
15. W.L. Hansen, S.J. Pearton and E.E. Haller, Appl. Phys. Lett. 44 (1984) 606.
16. J.I. Pankove, P.J. Zanzuchi and C.W. Magee, Appl. Phys. Lett. 46 (1985) 421.